8.4 Optical alignment system

For optimal performance of the muon spectrometer [131] over the entire momentum range up to 1 TeV, the different muon chambers must be aligned with respect to each other and to the central tracking system to within a few hundred μm in $r\phi$. The required alignment precision for the endcap chambers is 75–200 μm, while for the barrel the precision varies from 150 μm for the inner chambers of Station 1 to 350 μm for the outer chambers of Station 4. To this end, after following strict chamber construction specifications, CMS combines precise survey and photogrammetry measurements, measurements from an opto-mechanical system, and the results of alignment algorithms based on muon tracks (both from cosmic rays and from pp collisions) crossing the spectrometer.

There are several potential sources of misalignment in the muon spectrometer, from chamber production to final detector operating conditions, including:

- Chamber construction tolerances. These are unavoidable geometrical tolerances in the production of the chamber parts, such as mis-positioning of wires or strips within a layer and relative shifts in the layer-superlayer assembly. The relative positioning of the different internal components of a chamber was measured during construction to be within the required tolerances (Sect. 8.1 and 8.2). After assembly, all chambers were tested with cosmic muon data and showed good correlation between those measurements and the results of muon track fits. Furthermore, the geometry of the DT chambers was measured at the CERN ISR assembly hall using optical and survey techniques. These data are compared with construction drawings and cosmic data to provide corrections to the nominal chamber geometry when necessary.

- Detector assembly, closing tolerances. Gravitational distortions of the return yoke lead to static deformations of the steel support. This effect, together with the installation tolerances, results in displacements of the chambers in the different barrel wheels and endcap disks of up to several millimetres with respect to their nominal detector positions. After chamber installation, survey and photogrammetry measurements were performed for each wheel and disk. These measurements provide an initial geometry—position and orientation of each muon chamber in the different yoke structures—which absorbs installation tolerances and static steel deformations [175].

- Solenoid effects. Magnetic field distortions lead to almost perfect elastic deformations of the return yoke, at the level of a few centimetres. They result in further displacement of the chambers. The new detector geometry resulting from the magnetic forces is accessed with measurements of the optical system and track-based alignment techniques.

- Time-dependent effects. During operation, thermal instabilities and other time-dependent factors can cause dynamic misalignments at the sub-millimetre level.

The Muon Alignment (MA) system was designed to provide continuous and accurate monitoring of the barrel and endcap muon detectors among themselves as well as alignment between them and the inner tracker detector. To fulfil these tasks the system is organized in separate blocks: local systems for barrel and endcap muon detectors to monitor the relative positions of the chambers, and a link system that relates the muon and central tracker systems and allows simultaneous monitoring of the detectors.

The system must generate alignment information for the detector geometry with or without collisions in the accelerator. The dynamic range of the system allows it to work in the solenoidal magnetic field between 0 and 4 T. Its goal is to provide independent monitoring of the CMS tracking detector geometry with respect to an internal light-based reference system. This will help to disentangle geometrical errors from sources of uncertainty present in the track-based alignment approach, e.g., knowledge of the magnetic field, material description, and drift velocity.

The basic geometrical segmentation consists of 3 r-z alignment planes with 60° staggering in ϕ. This segmentation is based on the 12-fold geometry of the barrel muon detector. Within each plane, the 3 tracking sub-detectors of CMS (central tracker, barrel and endcap muon detectors) are linked together. Figure 214 shows schematic longitudinal and transverse views of CMS, with the light paths indicated. Furthermore, the barrel and endcap monitoring systems can work in stand-alone mode, in which they provide reconstruction of the full geometry of each independent sub-detector. The layout of the optical paths allows the monitoring of each of the 250 DT chambers, while only one sixth of selected CSCs in the 4 endcap stations are directly monitored. Alignment sensors located in the region between the muon barrel wheels and endcap disks allow the tracker and muon detectors to be aligned with respect to each other.

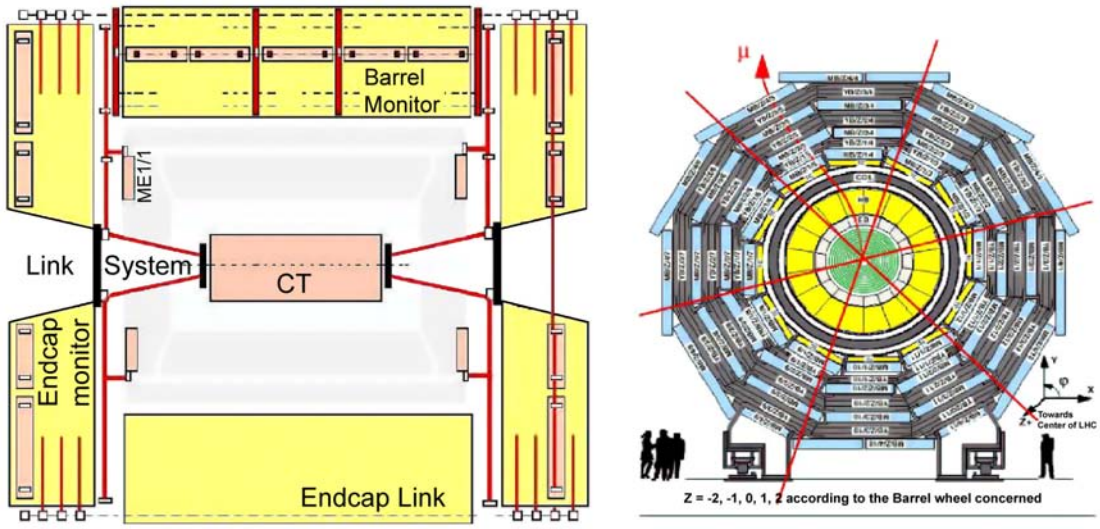

Figure 214: Schematic view of the alignment system. Left panel: longitudinal view of CMS. The continuous and dotted lines show different optical light paths. Right panel: transverse view of the barrel muon detector. The crossing lines indicate the r-z alignment planes with 60° staggering in ϕ.

8.4.1 System layout and calibration procedures

The optical network uses two types of light sources: LEDs and laser beams. It is composed of 10 000 LEDs and 150 laser beams together with precise measuring devices: $\approx$ 900 photo-detectors and $\approx$ 600 analog sensors (distance sensors and inclinometers), complemented by temperature, humidity and Hall probes. The system is structured into three basic blocks whose main features are described below.

Muon barrel alignment The monitoring of the barrel muon detector (Fig. 215) is based on the measurement of all the 250 DT chamber positions with respect to a floating network of 36 rigid reference structures, called MABs (Module for the Alignment of Barrel). The MAB design was optimised to achieve adequate mechanical rigidity of the structures under load and in thermal and humidity gradients. Long term measurements showed deviations below 100 μm and 50 μrad [176]. The MABs are fixed to the barrel yoke forming 12 r-z planes parallel to the beam line and distributed in ϕ every 60°. Each structure contains 8 specially designed video cameras that observe LED sources mounted on the DT chambers. Extra light sources and video-cameras in specific MABs serve to connect MABs in different planes forming a closed optical network (called diagonal connections). The MAB positions in the z coordinate are measured with respect to 6 calibrated carbon-fibre bars (z-bars) sitting on the outer surface of the vacuum tank of the solenoid. The MABs in the external wheels, YB$\pm$2, are equipped with extra alignment sensors and light sources that connect the barrel monitoring system with the endcap and tracker detectors.

The 4 corners of the DTs are equipped with LED light sources. Four LED-holders, or forks, are rigidly mounted on the side-profile of the honeycomb structure (2 per side) and use the rectangular 50 $\times$ 65 mm^2 tube as a light passage. Each fork contains 10 LEDs, 6 and 4, respectively, on each side. There are 10 000 light sources mounted on the DT chambers. The position of the forks with respect to the chamber geometry was measured on a dedicated bench with a precision of < 70 μm. As an important by-product, the calibration also provides the full geometry, including the planarity, trapezoidity, and the relative positions of superlayers for each DT chamber with < 40 μm precision, as described in Sect. 8.1.4. Each LED-holder and video-sensor was individually calibrated before its assembly on the DT chambers or MABs and z-bars. LED-holders were measured and the position of the light centroid was determined with respect to the holder mechanics with an accuracy of 10 μm. Long term measurements showed good stability of the centroids and light intensity distributions. CMOS miniature video sensors, containing

384×288 pixels with 12×12 μm^2 pixel size, were calibrated to absorb residual response non-uniformities and the intensity nonlinearities. The video cameras, consisting of a video sensor and a single-element lens assembled in an aluminium box, were also calibrated to determine their inner geometrical parameters. Fully instrumented MABs containing the necessary number of survey fiducials were calibrated on a special bench, where the whole geometry of the structure, positions, and orientations of elements were determined with overall accuracies of 70 μm and 50 μrad.

Once MABs were installed (Fig. 216), the initial MAB positions on the barrel wheels were determined by photogrammetry measurements.

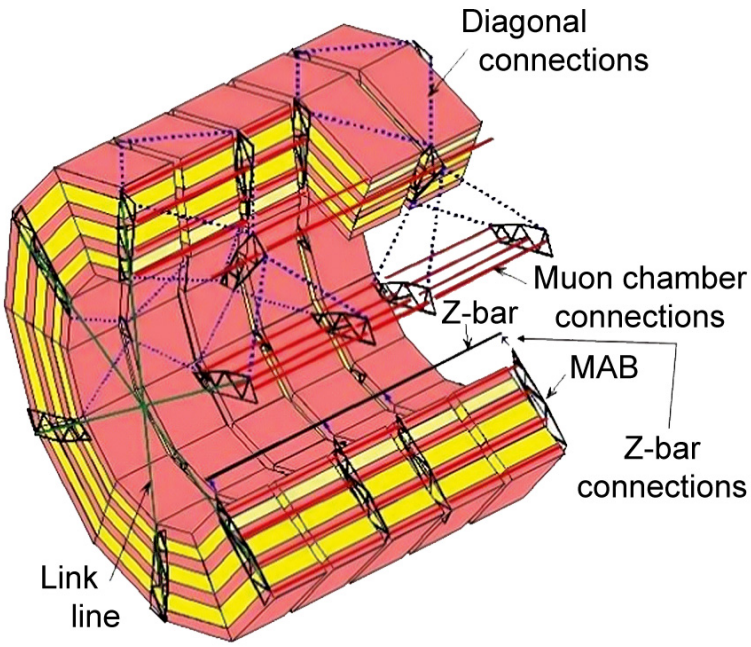

Figure 215: Schematic view of the barrel monitoring system showing the optical network among the MAB structures.

The control, read-out, and data preprocessing [177] are performed by a network of local minicomputers (1 per MAB, 36 in total) that makes it possible to run the full system in parallel. The minicomputers are connected to the main control PC via an Ethernet network capable of working in magnetic fields. The main control PC synchronises the operation of the light sources mounted on the DT chambers and the read-out of the images taken by the cameras. The minicomputers control the light sources mounted on the MABs and the z-bars, read out the temperature and humidity sensors, perform the image read-out and digitisation, and calculate the image centroids of the light sources. The results are transferred to the main control PC, which is connected to the corresponding central CMS units.

Based on simulation, the barrel monitoring system should provide a stand-alone measurement of the barrel chambers with an average r-ϕ position accuracy of 100 μm for chambers in the same sector and about 250 μm between barrel sectors. The current understanding of its performance is discussed in Sect. 8.4.3.

Muon endcap alignment The muon endcap alignment system [178] is designed to continuously and accurately monitor the actual positions of the 486 CSCs relative to each other, relative to the tracking system, and ultimately within the absolute coordinates of CMS. Due to the large magnetic field, the chambers mounted on the endcap yoke undergo substantial motion and deformation, on the order of a few centimetres, when the field is switched on and off. The alignment system must measure the disk deformation and monitor the absolute positions of the CSCs in the r-ϕ plane and in z. From simulations, the required absolute alignment accuracies were found to run from 75 to 200 μm in r-ϕ. Because the r and r-ϕ accuracies are directly coupled, the required accuracy in the r-position is $\approx$400 μm. The z displacement due to the deformation of the iron yoke disks caused by the strong and non-uniform magnetic field in the endcaps requires the alignment sensors to be able to accommodate a dynamic range of $\approx$2 cm

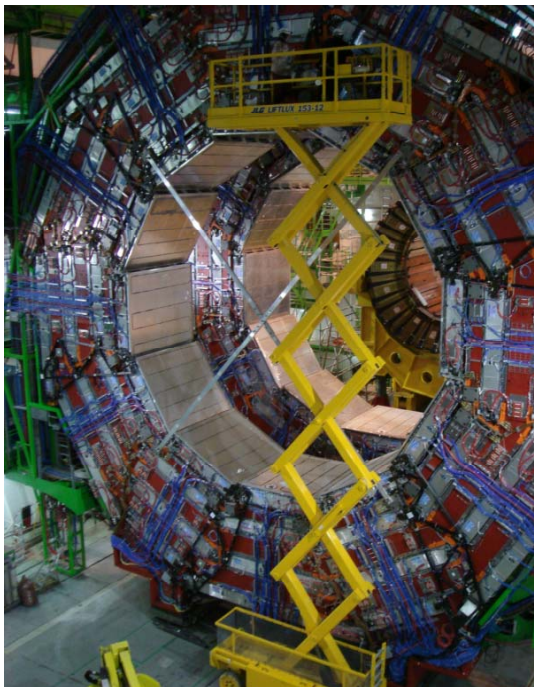

Figure 216: Installation of the MABs on wheel YB+2.

with an accuracy of ≈1 mm.

The system uses a complex arrangement of 5 types of sensors for the transferring and monitoring of ϕ, r, and z coordinates (Fig. 217). The system measures one sixth of all endcap chambers. The main monitoring tools within the r-ϕ plane are the Straight Line Monitors (SLM). Each SLM consist of 2 cross-hair lasers, which emit a nearly radial laser beam across 4 chambers from each end, and provide straight reference lines that are picked up by 2 optical sensors (Digital CCD Optical Position Sensors, DCOPS [179]). This arrangement provides references for the chamber positions relative to the laser lines. Figure 218 shows a photograph of a complete SLM on station ME+2. The figure also indicates r-sensors for monitoring radial chamber positions, z-sensors for axial distance measurements between stations, and a clinometer for monitoring the tilt of the mechanical support assembly (transfer plate) onto which lasers, reference DCOPS, and z-sensors are mounted. The inset in Fig. 218 shows the location of proximity sensors on the outer ring of the ME+1 station, which monitor the azimuthal distance between neighbouring chambers. These are necessary because the outer ring of ME1 chambers is the only ring for which the CSCs do not overlap in ϕ. Furthermore, every CSC and alignment device is equipped with photogrammetry targets to allow absolute magnet-off measurements.

The ϕ coordinate alignment is handled by optical SLMs and transfer lines. Transfer laser lines run parallel to the CMS z-axis along the outer cylindrical envelope of CMS at 6 points separated by 60° in ϕ. The SLMs run across the surface of one sixth of all the CSCs, along radial directions, and link transfer lines on opposite sides of a disk. Both laser lines have a similar basic configuration: a laser beam defines a direction in space that is picked up by several DCOPS precisely mounted on CSCs or transfer plates to reference their own positions. Mounting accuracies due to tolerances of dowel pins and dowel holes are ≈50 μm. Every DCOPS comprises 4 linear CCDs, each with 2048 pixels and 14 μm pixel pitch. The CCDs are basically arranged in the shape of a square and can be illuminated by cross-hair lasers from either side. The r and z coordinate measurements are performed by analog linear potentiometers and optical distance devices in contact with aluminium tubes of calibrated length.

All analog sensors were calibrated with a 1D precision linear mover with 6.4 μm step size. The uncertainty in the absolute distance calibration is 100 μm for r sensors and 53 μm for z sensors [180]. Calibration for optical DCOPS consisted in determining the distance from the surface of the mount hole for a reference dowel pin to the first active CCD pixel and measuring the projected pixel pitch of each of the 4 CCDs. This was done on a calibration bench where a fibre-bundle variable light source at the focus of a parabolic mirror illuminated a mask with 8 optical slits. A simple geometry reconstruction, based on coordinate-measuring-machine data for the calibration mask and sensor mounts, determined the physical pixel positions. Calibration errors were typically 30 to 50 μm.

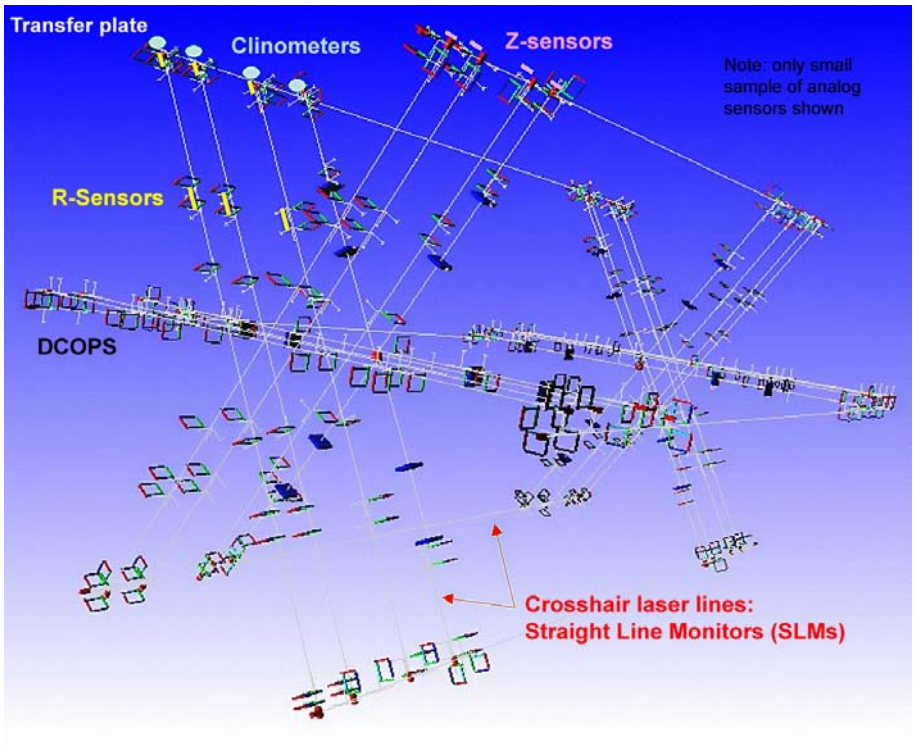

Figure 217: Visualisation of the geometry and components of the muon endcap alignment system. The square objects represent optical sensors (DCOPS) for monitoring 3 straight laser lines across each endcap station.

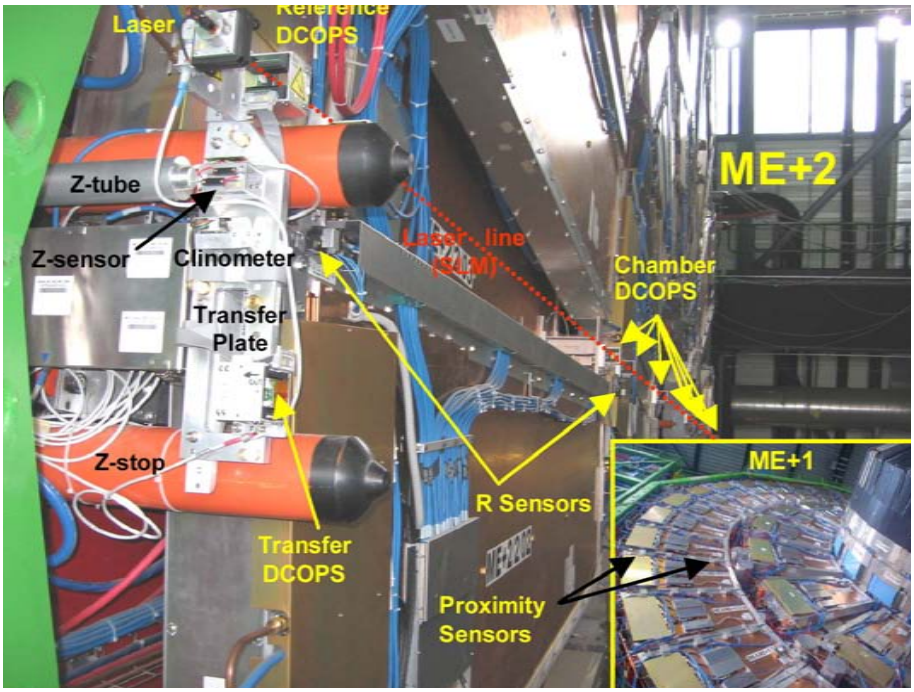

Figure 218: Close-up of one of the 3 Straight Line Monitors (SLM) on the ME+2 station with cross-hair laser, DCOPS, and analog sensors (r, z, and Tiltmeter). The insert indicates the location of proximity sensors on ME+1.

Link system The purpose of the link alignment system is to measure the relative position of the muon spectrometer and the tracker in a common CMS coordinate system. It is designed to work in a challenging environment of very high radiation and magnetic field, meet tight space constrains, and provide high precision measurements over long distances. A distributed network of opto-electronic position sensors, ASPDs (amorphous-silicon position detectors) [181], placed around the muon spectrometer and tracker volumes are connected by laser lines. The entire system is divided into 3 ϕ-planes 60° apart; this segmentation allows a direct reference of each muon barrel sector with the tracker detector and provides a direct reference also to the endcap alignment lines in the first endcap station, ME1. Each plane consists of 4 quadrants (Fig. 214) resulting in 12 laser paths: 6 on each z-side of the CMS detector, and generated by 36 laser sources. The system uses 3 types of reference structures: rigid carbon-fibre annular structures placed at both ends of the tracker (alignment rings, AR) and at the YE$\pm$1 wheels of the endcap muon spectrometer (link disks, LD); and the MAB structures attached at the external barrel wheels, YB$\pm$2. Figure 219 (left) shows the LD and AR carbon fibre structures installed in the inner η = 3 cone. The link measurement network is complemented by electrolytic tiltmeters, proximity sensors in contact with aluminium tubes of calibrated length, magnetic probes, and temperature sensors.

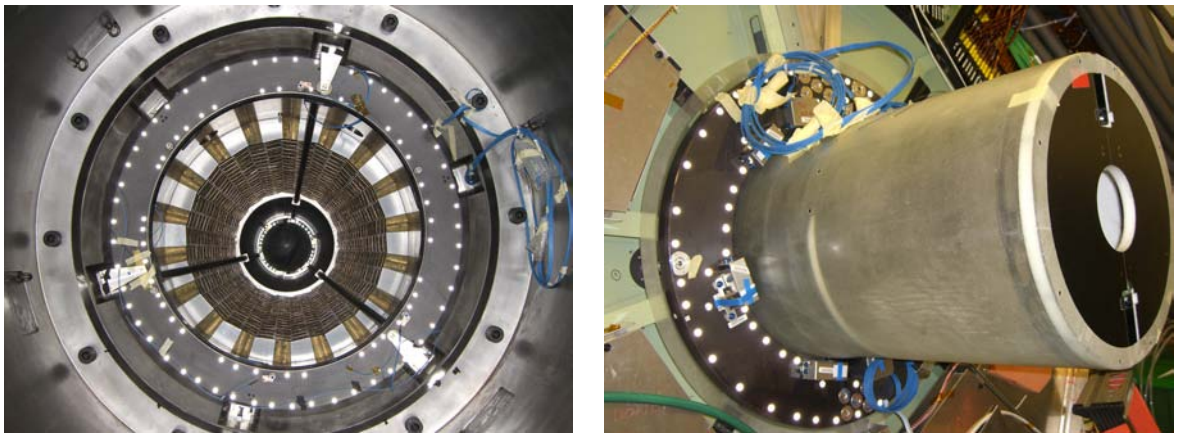

Figure 219: Left panel: Link Disk and Alignment Ring installed in the inner η = 3 cone during the first closing of the detector in summer 2006, MTCC period. Right panel: Alignment Ring mounted in the TEC end flange.

The ARs are rigidly attached to the endcap tracker detectors, TECs, through a purely mechanical connection with the instrumented silicon volume (Sect. 4.3.7). Three pillars, acting as support fixations, connect the last instrumented disk of each TEC with the corresponding AR, at both ends of the tracker volume, see Fig. 219 (right). The position and orientation of the ARs with respect to the TEC disks 9 and 10 were measured with a coordinate-measurement machine using the external survey fiducials prior to the TEC assembly and instrumentation. Changes in angular orientations are monitored by high precision tiltmeters placed at the AR and TEC disk 10. Laser sources originating at the AR and running along the inner detector boundary reach ASPD sensors on the first endcap disk, ME1, and on the external barrel wheel.

The ASPDs are 2D semitransparent photo-sensors, which consist of 2 groups of 64 silicon micro-strips with a pitch of 430 μm oriented perpendicularly. With $\geq$80% transmittance for the 685 nm wavelength used in the system, they allow multi-point measurements along the light path without significant distortions in the beam direction. The intrinsic position resolution is about 2 μm. The location, centre position, and orientation of the ASPD with respect to reference pins in their mechanical mount are measured with a non-contact CMM (Coordinate Measuring Machine) with an overall accuracy of 15 μm. Distance measurement devices (optical distance sensors and linear potentiometers) already mounted in their final mechanics were calibrated using 2 μm resolution linear movers and pre-measured calibration fixtures. The uncertainties in absolute and relative calibration [182] are below 50 μm and 20 μm, respectively, for the different sensor types. The intrinsic accuracy of the tiltmeters sensors, after calibration, is about 2 μrad; mechanical offsets inherent to the mechanical mounts and assembly tolerances are determined by survey and photogrammetry techniques.

The light sources (collimators) and specific optical devices housed on the alignment reference structures (AR, LD, and MABs) create the laser beam paths with the layout described above. Each collimator is focused to its working distance to ensure Gaussian beam profiles along the propagation path to avoid beam-shape-induced bias in the position reconstruction. The adjustment and calibration [183] of the laser rays for the AR and LD structures were done on a dedicated bench instrumented with a precise survey network that mimics the nominal detector geometry.

Beams were adjusted to their nominal geometry with a precision better than 100 μrad. Long term measurements were performed after beam adjustments. Beam pointing stability, including temperature effects, was found to be better than 30 μrad. The adjustment and calibration accuracy was limited to 30–100 μrad due to the finite dimension of the structures combined with the intrinsic accuracy of the survey and photogrammetry measurement techniques of 70 μm.

Survey and photogrammetry measurements are also performed during the installation of the alignment structures in the detector. An installation accuracy of the order of a few millimetres and milliradians is needed to ensure correct functionality of the system, taking into account the standard CMS assembly tolerances of the big endcap disks and barrel wheels.

The control, read-out, and data preprocessing are performed by two types of electronic boards. Analog sensors read-out and laser control use standard ELMB (embedded local monitor board) cards [184]. For the read-out of ASPD sensors, custom made LEB (local electronic board) cards were developed. LEBs are intelligent imaging acquisition boards made to read and control up to 4 ASPD sensors. They are based on Hitachi micro-controllers. ELMB and LEB boards use the CAN communication protocol to connect the front-end electronics and the main control PC unit.

8.4.2 Geometry reconstruction

The DAQ, monitoring, and control software are integrated into the DCS (detector control system) environment. Data are recorded in an online Oracle database and subsequently converted into ntuples by specialised programs that perform database queries and apply calibrations to convert raw values into meaningful physical quantities. This provides the necessary information for global geometry reconstruction, which is handled by COCOA (CMS Object-Oriented Code for Optical Alignment) [185], an offline program to simulate and reconstruct the complex optical alignment system. Due to the unknown movements of different CMS structures, the sensors of the optical alignment systems will not measure the expected nominal values. The aim of COCOA is to analyse the observed changes in these measurements to determine which are the displacements and/or rotations that caused them. The approach adopted by COCOA to tackle this problem is to solve the system of equations that relate the measurement values to all the positions, rotations, and internal parameters of all the objects that make up the system. In fact, to solve the system of equations, one does not need to know the explicit form of the equations, but only the derivatives of each measurement value with respect to each object parameter. COCOA uses a geometrical approximation of the propagation of light to calculate numerically these derivatives and then solves the system of equations through a nonlinear least squares method. Due to the large number of parameters in CMS (about 30 000), big matrices are needed. COCOA matrix manipulations are based on the Meschach Library [186].

COCOA has proved its robustness through its extensive use in CMS for several design studies, as well as for the analysis of several test benches and magnet test results. Its output, the aligned geometry, will be used as input geometry for track reconstruction as well as for further alignment studies based on muon tracks from cosmic rays and from pp collisions.

8.4.3 System commissioning and operating performance

A first test of the large superconducting solenoid magnet in the CMS detector was successfully performed between June and November 2006, during which stable operation at full field (4 T) was achieved (Sect. 3.3). The alignment sensors, read-out, and DAQ software were commissioned during this test period for about one third of the system, instrumented at the $+z$ side of the detector. This allowed the first full-scale dynamic test of the system. The performance of the system as well as the main features of the yoke displacement and deformation were studied. The relevant results are summarised below:

- Measurement of relative movements due to thermal changes.
  The effects of thermal changes (day-night variations) for DT and CSC chambers were recorded for the conditions present during the test, with the detector in the surface assembly hall and power on only $\approx$5% of the muon spectrometer. The measured relative movement did not exceed 50 μm over the entire test period, with changes in position showing a good correlation with temperature. Although a movement of this magnitude is not relevant from the physics analysis point of view, its measurement illustrates the good resolution of the alignment system.
- Measurement of the displacements and deformations of the yoke structures.
  Two effects were observed. The first is the change in the original positions of the structures (the positions

before any magnet operation). The displacements of the structures along the z direction towards the solenoid seem to stabilise after the first 2.5–3 T are reached. This compression is permanent, meaning it is not reversed/recovered in subsequent magnet off states, and it is interpreted as the final closing of the structures due to the magnetic forces acting on the iron. These measured displacements are specific to the first CMS closing experience and cannot be extrapolated to other scenarios.

The second effect is the almost perfectly elastic deformations between magnet-on and magnet-off states, as illustrated in Fig. 220. At 4 T, the elastic deformation of the barrel yoke, measured at the end of the $+z$ side with respect of the plane of the interaction point, is about 2.5 mm. Figure 220 shows the elastic compression of the barrel wheels versus the magnet current as recorded in the second phase of the Magnet Test period. Despite the large overall compression of the barrel spectrometer, an important measurement was the stability of the barrel chambers during the whole data-taking period. The relative movements in the r-ϕ direction did not exceed 60 μm.

The behaviour of the endcap disk is more complicated. Due to the strong gradient in the magnetic field near the end of the solenoid, strong magnetic forces pull the central portions of the endcap disks towards the center of the detector. As shown in Fig. 220, the nose is pulled towards the interaction point, the magnitude of the compression is perfectly correlated with the magnet current, reaching up to $\approx$16 mm at 4 T. The various z-stops, which prevent the disks from getting pushed into each other and onto the barrel wheels, cause the endcap disks to bend into a cone shape. The z-stops between endcap and barrel, positioned at nearly half the disk radius, cause the side of the YE1 disk facing the barrel to compress radially around them by $\approx$600 μm, while expanding azimuthally by $\approx$800 μm. This explains the radial compression of the face of ME+1 and the larger bending angles at mid-radius than at the outer edge (Fig. 221). Endcap disk deformations are predicted by finite element analysis (FEA) using the ANSYS program [3]. The measurements are in reasonable quantitative agreement for all displacements and deformations, as shown in Fig. 221. Note that the front z-stops, between the ME1 and barrel wheels, were not included in the FEA, which explains the difference. The difference between top and bottom is also explained by the presence of the carts that support the disks.

The rest of the endcap stations on YE+2 and YE+3 experience a maximum bending angle of $\approx$2.5 mrad relative to the vertical, as sketched in Fig. 222. As in the case of the barrel chambers, with stable 4 T field, the observed relative movements were very small.

- Detector closing tolerances and reproducibility.
  The test of the magnet was divided into 2 phases, separated by a short period during which the yoke was open to extract the inner detectors, tracker, and ECAL modules. This allowed a test of the reproducibility in the closing procedure and tolerances, as well as the study of the compatibility of measurements between the two phases. Reproducibility in the closing was at the level of a few millimetres for the barrel wheels and about an order of magnitude higher for the endcap disks. The particular conditions of the test did not allow the establishment of a solid understanding of reproducibility for the process of closing the different structures. Instead, the system was able to reproduce the same magnetic-force-induced effects as measured in the first period.

From this test we conclude that the system operates adequately under magnetic fields both in terms of dynamic range and measurement performance. The system precision achieved is $\leq$ 300 μm and the measurement accuracy has been validated against results from photogrammetry and cosmic ray tracks.

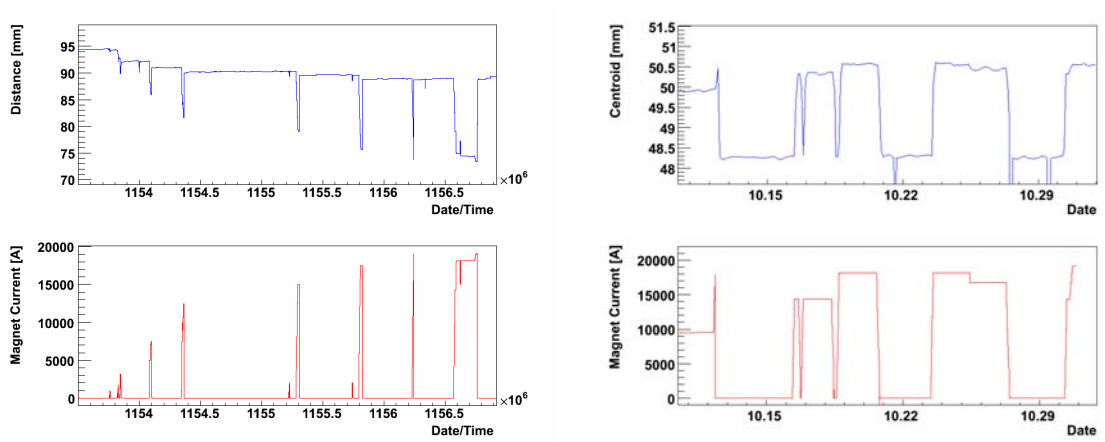

Figure 220: Deformations of endcap disks and barrel wheels vs magnet current cycling. Left panel: The bottom plot shows the magnet powering cycle exercised during the first phase of the Magnet Test period. The top plot shows the measured YE+1 nose compression towards the interaction point. Right panel: The bottom plot shows the magnet powering cycle exercised during the second phase of the Magnet Test period. The top plot shows the calculated approximate YB+2 compression towards the interaction point.

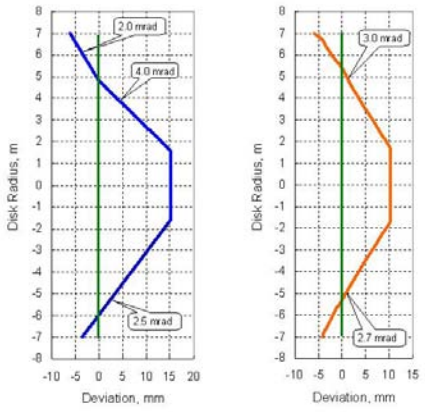

Figure 221: Comparison of the YE+1 disk deformations in the r-z plane at full magnetic field (4 T) measured by the alignment system (left panel) and predictions from finite element analysis (right panel). The vertical lines correspond to 0 magnetic field.

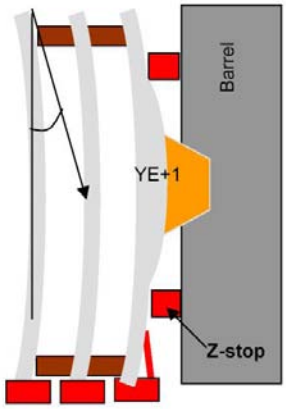

Figure 222: Current understanding of disk deformation due to magnetic forces based on alignment system measurements. The z-stops (red) prevent the disks from getting pushed into each other. Note that the indicated bending angle is exaggerated for illustrative purposes. Its measured magnitude is 2.5 mrad.